

FORCED CONVECTION HEAT TRANSFER IN A TURBULENT FLOW THROUGH A SQUARE DUCT

HIDEOMI FUJITA, MASAFUMI HIROTA
and HAJIME YOKOSAWA*

Department of Mechanical Engineering

(Received October 31, 1988)

Abstract

An experimental study on forced convection heat transfer for a constant wall temperature was conducted in a turbulent flow through a square duct to examine the effects of the secondary flow of Prandtl's second kind on the temperature field of a flow in the duct. The wall heat flux distribution showed the minimum near the mid point of a wall and the maximum midway between the mid point of a wall and an adjacent corner. There were similarities between the contour map of mean temperature and that of primary flow velocity: there were bulges toward corners along corner bisectors and depressions toward the duct center along wall bisectors. The mean temperature distributions measured along lines normal to a wall in the region near the mid point of the wall were well described with the inner law.

1. Introduction

The secondary flow of Prandtl's second kind is generated in turbulent flows in non-circular straight ducts, the kind of which is often encountered in engineering practice. Although the secondary flow velocities are only a few percent of the streamwise bulk velocity, the secondary flow greatly affects the flow characteristics. The authors have conducted measurements of the turbulent flows in the same rectangular ducts with and without roughened walls, and reported that (1) different patterns of secondary flow were observed in a duct, depending on the roughness of the wall, and (2) the magnitude of the

* College of General Education, Nagoya University

secondary flow in a duct with rough walls is bigger than that in a duct with smooth walls.¹⁾⁻³⁾ Although, in ducts with rough walls, the secondary flow would affect the characteristics of the forced convection heat transfer (as has already been observed for its effects on the characteristics of the flow field), there are only few reports on the measurement of temperature field even in a square smooth duct which can be regarded as a fundamental duct.⁴⁾ As a first step to definitely showing the effects of the secondary flow on the turbulent heat transfer in rectangular ducts, this report is concerned with the turbulent flow in a smooth square duct, which can be regarded as the most fundamental flow. Due to lack of useful data on temperature field measurement, we conducted such measurements, the results of which are presented here in order to examine the effects of the secondary flow on the temperature field in the duct.

2. Experimental Apparatus

Fig. 1 is a scheme of the experimental apparatus. Air at room temperature is introduced to the test duct after flowing through a quadrant flow nozzle and a settling chamber. The test duct has a square cross-section with a side length of $D=2B=50\text{ mm}$

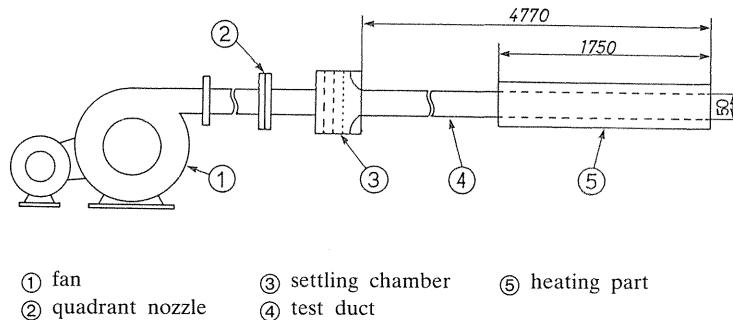


Fig. 1. Experimental apparatus.

and is 4770 mm in length. The duct includes a heating part which has a structure of a double-duct and is between the duct exit and 1750 mm upstream from the exit. The outer and inner ducts of the heating part were made of Bakelite plate and 1 mm thick brass plate, respectively. Saturated steam at atmospheric pressure flows through the passage between the inner and outer ducts and heats isothermally the whole wall of the inner duct so as to maintain a temperature of about 373K. 52 thermocouples mounted on the outer surface of the inner duct wall served to verify that the condition of an isothermal wall was satisfied. Measurements were conducted at the cross-section 100 mm upstream from the duct exit (which is $93.4D$ downstream from the test duct entrance and $33D$ downstream from the heating part entrance) where both velocity and temperature fields can be considered to be fully developed. Reynolds number $Re=UD/\nu$ evaluated on the condition at the entrance of the heating part was kept at 6.5×10^4 . According to the Metz-Eckert chart,⁵⁾ the present experiment falls in the category of forced convection, turbulent flow. Accordingly the effect of free convection can be neglected. For the measurements of air

temperature, a resistance thermometer with a tungsten wire sensor ($5\ \mu\text{m}$ in diameter and $1\ \text{mm}$ in length) was used. Since the thermometer operates on a constant current as small as $1\ \text{mA}$, overheat of the sensor was so low that the sensor velocity sensitivity was negligible.⁶⁾ As for the frequency response of a resistance thermometer, it is by far improved relatively to a thermocouple thermometer. The resistance thermometer, however, can not respond to extremely rapid change in temperature owing to the heat capacity of its sensing wire⁷⁾: it is estimated that the sensor used in the measurements has the frequency ranges up to about $400\ \text{Hz}$ in a flow of $20\ \text{m/s}$ and about $150\ \text{Hz}$ in the still air. The upper limit of these frequency ranges are not large enough to measure the fluctuating temperature accurately, and in principle, they can be extended to higher values by the use of a finer wire. In the present experiment, the tungsten wire of $5\ \mu\text{m}$ in diameter is used, which is currently regarded as the best sensor in all obtainable ones from the view points of both sensitivity and strength. The thermometer was calibrated statically in an air flow of $20\ \text{m/s}$, a velocity which was almost the same as the bulk mean velocity in the test duct, within an accuracy of $\pm 0.06\ \text{K}$.

3. Experimental Results

3.1. Average Nusselt number

Fig. 2 shows the average Nusselt number $Nu = hD/k$ as a function of the Reynolds number. $h = Q/A\Delta T$ stands for the mean heat transfer coefficient on the basis of log-mean temperature difference. Q stands for the total heat added to air, and is evaluated in terms of an enthalpy difference between the outlet and inlet of the heating part of the test duct.

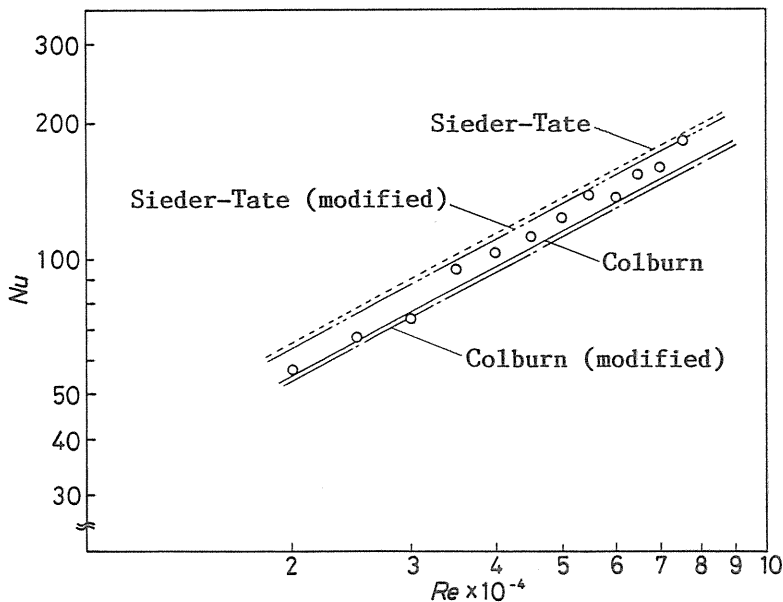


Fig. 2. Average Nusselt number.

In Fig. 2, $\log Nu$ increases with the increase of $\log Re$ linearly, and correlation can be expressed by the following relation:

$$Nu = 0.0221 Re^{0.8} \quad (1)$$

Empirical relations, recommended by Colburn,⁸⁾ and Sieder and Tate,⁹⁾ for fully developed turbulent flow in circular tubes at constant wall temperature are shown in the figure. The relations are shown for a case where the hydraulic diameter is used and for a case where the modified hydraulic diameter calculated by using the way recommended by Brundrett¹⁰⁾ is used. Plots are in the region bounded by the lines showing the empirical relations. This shows that the empirical relations for circular tubes can be applied to a square duct with sufficient accuracy by the straightforward use of the hydraulic diameter.

3. 2. Local wall heat flux distribution

In this experimental study, thorough measurements of temperature distributions near the wall surface were conducted to obtain accurately the local wall heat flux. Examples of

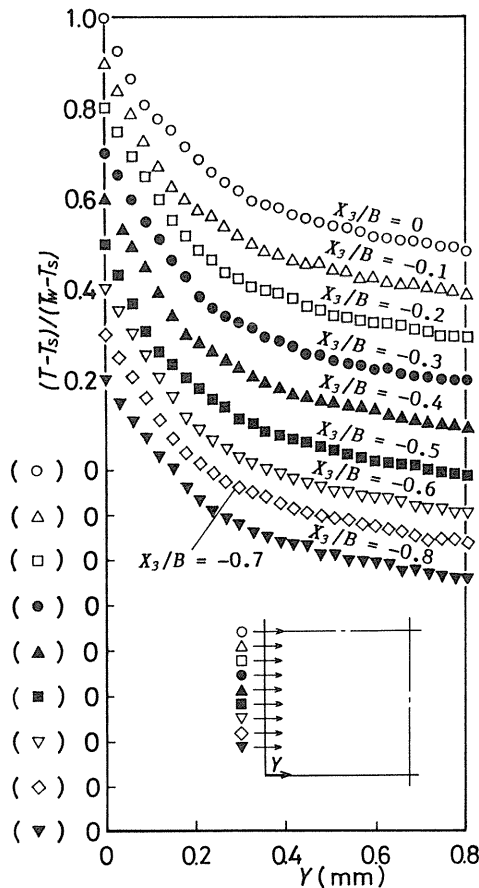


Fig. 3. Mean temperature profiles in near-wall region.

the results are shown in Fig. 3. In the measurements, a temperature probe was traversed from $Y=0$ to $Y=0.8\text{ mm}$ at an interval of 0.03 mm , where $Y=0.8\text{ mm}$ corresponds to $Y^+=YU^*/\nu\approx 50$.

In the region close to the wall where $Y<0.2\text{ mm}$, or $Y^+<13$, the mean temperature decreases straight toward the center of the duct, that is each temperature distribution makes a straight line within the region. While in the region where $Y>0.2\text{ mm}$, the slope decreases rapidly with Y . Each mean slope of the distribution in the region $Y<0.2\text{ mm}$ was calculated by using the least squares method to obtain wall heat flux $q_w=-k(dT/dY)_w$. Distribution of q_w is shown in Fig. 4. q_w is an averaged value of several measurements repeated at the same location and shown in the figure by the ratio to the mean heat flux \bar{q}_w obtained by the circumferential integration. The experimental results obtained by Brundrett and Burroughs⁴⁾ (represented by a solid line) and the results of numerical analysis obtained by Fujita et al.³⁾ (represented by a dashed curve) are brought in the figure for comparison. The results of the present experiment agree very well with their results. Results of wall shear stress, $\tau_w/\bar{\tau}_w$, measured in the isothermal flow¹⁾ are also shown in Fig. 4. As can clearly be seen, distribution profile of q_w is similar to that of τ_w . q_w has the minimum value near the mid point of a wall, increases with the decrease in X_3 to attain maximum at $X_3/B=-0.5$, and decreases gradually toward corners of the duct.

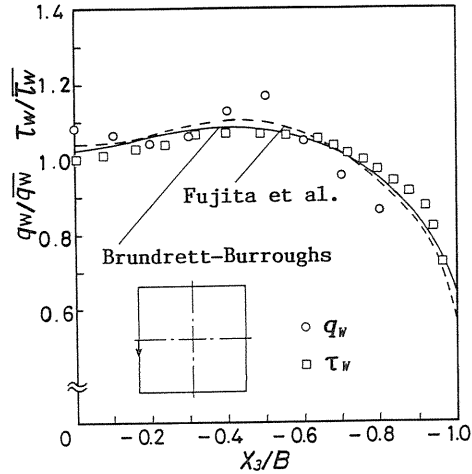


Fig. 4. Local wall heat flux.

3. 3. Temperature distribution in a duct cross-section

Fig. 5 shows mean temperature profile in half of the duct cross-section. Distribution profiles at $X_3/B=0$ and -0.2 are similar to a parabola in which $(T_w-T)/(T_w-T_s)$ is proportional to $(Y/B)^{0.242}$. In decreasing X_3/B and when the wall is approached, the profiles deviate from the parabolic distribution. When $X_3/B<-0.6$, T_w-T shows its minimum at $X_2/B=0$ and maximum at $X_2/B=\pm 0.5$.

The temperature distribution has a strong resemblance to the primary velocity distribution shown in Fig. 6.

Fig. 7 shows the contour map of the mean temperature. Contours have bulges toward corners along corner bisectors and depressions toward the duct center along wall bisectors. Distortions in contour lines are more prominent in the near wall region where $|X_2/B|>0.5$ and $|X_3/B|>0.5$. The distortion observed in the contour map of Fig. 7 corresponds closely to the secondary flow vectors diagram¹⁾ shown in Fig. 9. The bulge of contours shows that the secondary flow transports low temperature fluid from the core to the corners of the duct, and, near the mid point of a wall, the secondary flow which proceeds along the wall bisectors transports high temperature fluid from the close vicinity of the walls to the duct center. This results in the depression of contour lines. Therefore the effects of the secondary flow on the distribution profile of mean temperature may appear pronounced in

the region near duct walls. In addition, the distribution of q_w/\bar{q}_w , shown in Fig. 4, can be illustrated by the distortions in the contours of the mean temperature caused by the secondary flow.

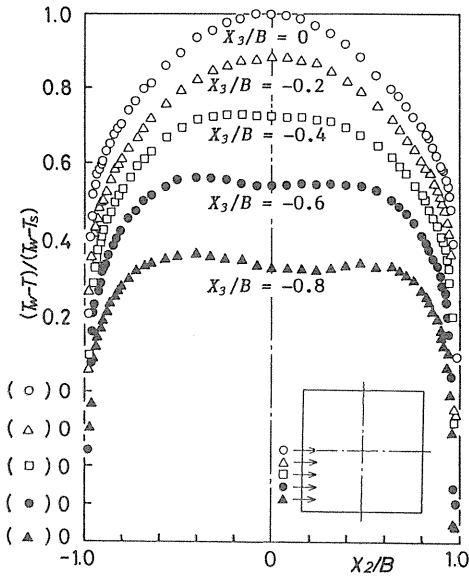


Fig. 5. Mean temperature profile.

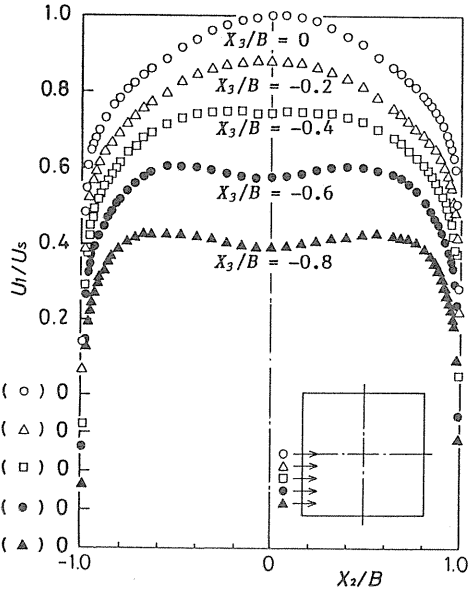


Fig. 6. Mean primary flow velocity profile.

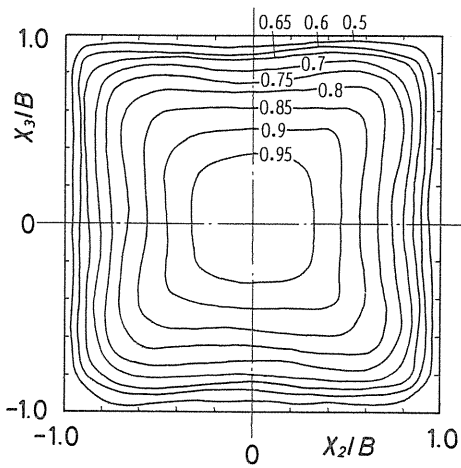


Fig. 7. Mean temperature $(T_w - T)/(T_w - T_s)$.

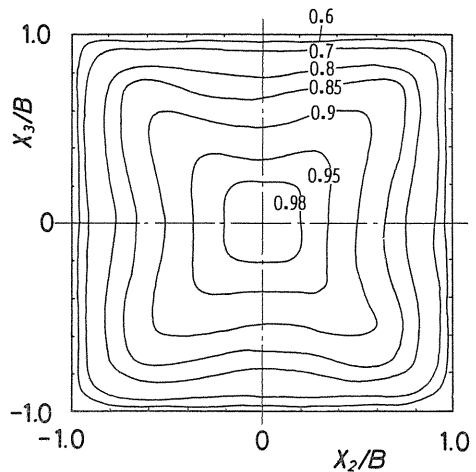


Fig. 8. Mean primary flow velocity U_1/U_s .

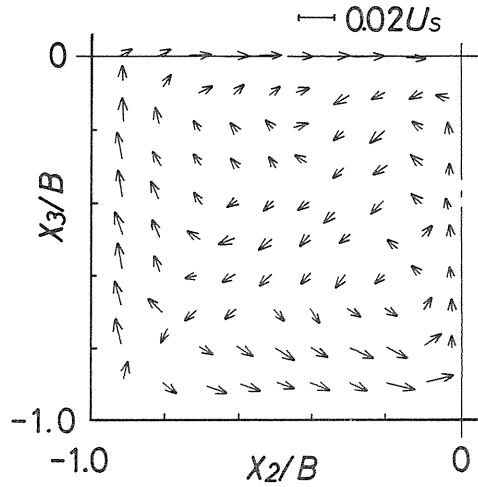


Fig. 9. Secondary flow vectors.

Fig. 8 shows the contour map of the mean primary flow velocity measured for an isothermal flow in the same duct. The contour map of the mean temperature bears a close resemblance to that of the mean primary flow velocity. This suggests that there were similarities between the momentum transfer and heat transfer caused by the secondary flow. Further, the distribution of mean temperature obtained by the present experiments showed a good agreement with the results of numerical analysis conducted by Fujita et al.³⁾

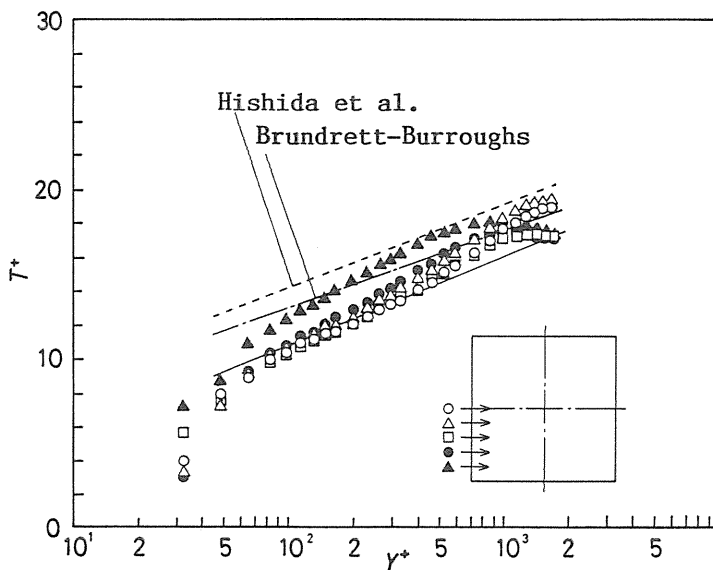


Fig. 10. Mean temperature in wall coordinate.

The universal temperature profiles are shown in Fig. 10. In the region at $X_3/B > -0.4$, the region far from the corners, a relation between T^+ and Y^+ is expressed in the following logarithmic law at $Y^+ < 200$ where an inner law generally holds.

$$T^+ = 5.17 \log Y^+ + 0.33 \quad (2)$$

Although the evaluations by the above expression are smaller than the results of turbulent pipe flow reported by Brundrett and Burroughs,⁴⁾ and by Hishida et al.,¹¹⁾ agreement in the slope of these three results is fairly good. In the region at $X_3/B < -0.6$, temperature distribution deviates prominently from the logarithmic law. This is affected by the neighboring walls. In addition, the mean primary flow velocity profile in an isothermal flow is described by the expression given by Sarnecki as

$$U^+ = 5.5 \log Y^+ + 5.45 \quad (3)$$

in a relatively wide area.¹⁾

Fig. 11 shows a contour map of the intensity of fluctuating temperature in a duct cross-section. As stated above, owing to a time lag caused by a heat capacity of the

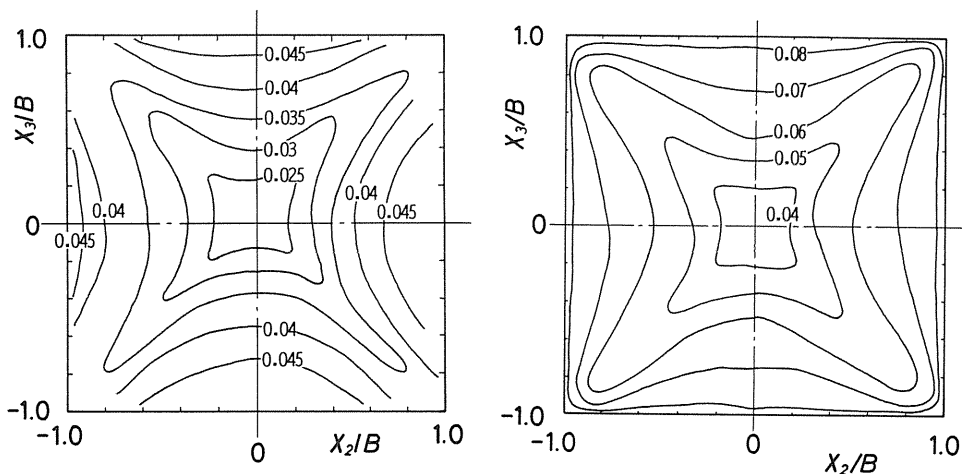


Fig. 11. Fluctuation temperature $\sqrt{\overline{t^2}}/(T_w - T_s)$. Fig. 12. Streamwise fluctuation velocity $\sqrt{\overline{u_1^2}}/U_s$.

sensing wire, a resistance thermometer does not respond correctly to the temperature fluctuation of extremely high frequency. Moreover, it is known that the gain of the resistance thermometer deteriorates rapidly in proportion to the increase in temperature fluctuation frequency.⁷⁾ Therefore, if examined quantitatively, it seems possible that the values of the fluctuating temperature intensity are somewhat smaller than the true values. Hence, as for Fig. 11, the authors restrain themselves from making quantitative discussion, and only qualitative features of the distribution are described in the following.

The profile of the intensity of fluctuation temperature is similar to that of the mean temperature. In particular, the bulges toward corners along the corner bisectors and

depressions toward the duct center along the wall bisectors in contours are more prominent than those of the mean temperature. The effects of the secondary flow appear more clearly on the distribution of the fluctuation temperature than that of the mean temperature. This tendency is quite the same as the relation between the contour map of the primary flow velocity and that of the streamwise fluctuation velocity of which the contour map is shown in Fig. 12. The form of fluctuation temperature contours is similar to that of the fluctuation velocity contours.

4. Conclusions

The experimental results as explained above lead to the following major conclusions:

- (1) Empirical relation between average Nusselt number, Nu , and Reynolds number, Re , was obtained to be $Nu=0.0221Re^{0.8}$.
- (2) The local wall heat flux, q_w , on a wall shows the minimum value near the mid-point of the wall, increases with the distance from the mid-point of the wall towards a corner, and decreases in approaching the corner after having attained a maximum at the central portion between the mid-point of the wall and the corner.
- (3) The contour lines of mean temperature have bulges towards corners along corner bisectors of the duct cross-section and depressions towards the axis of the duct along wall bisectors affected by the secondary flow. Similar trend to this is seen in the distribution of fluctuation temperature intensity. However, bulges and depressions are more prominent than the mean temperature distribution.
- (4) In the region near the mid point of a wall, mean temperature is well described with the temperature inner law at $Y^+ < 200$. But, in the region near a corner, mean temperature distribution deviates from the inner law.

Acknowledgement

The authors wish to express their appreciation to Mr. S. Kagami for his competent assistance in conducting the experiments. They also express their appreciation to Messrs. H. Kawamura, A. Fujishiro, and N. Shiraki for their kind help in making the experimental apparatus.

Notation

A	Heat transfer surface area.
$B=D/2$	Half length of a side.
C_p	Specific heat at constant pressure.
D	Side length of square duct.
h	Heat transfer coefficient.
k	Thermal conductivity.
$Nu=hD/k$	Nusselt number.
Q	Heat added to fluid.

q_w	Wall heat flux.
$Re=UD/\nu$	Reynolds number.
T	Time mean temperature.
$T^+=(T_w-T)/(q_w/\rho C_p U^*)$	Dimensionless temperature.
T_s	Time mean temperature at the center of a duct cross-section.
ΔT	Log-mean temperature difference.
U	Bulk mean velocity.
U^*	Friction velocity.
$U^+=U_1/U^*$	Dimensionless velocity.
U_1	Time mean velocity component in X_1 direction.
u_1	Fluctuation velocity component in X_1 direction.
U_s	Time mean velocity at the center of a duct cross-section.
X_1, X_2, X_3	Orthogonal co-ordinates.
Y	Distance from wall.
$Y^+=YU^*/\nu$	Dimensionless distance.
ρ	Density of fluid.
τ_w	Wall shear stress.
Subscript	
w	Values at the wall surface.

References

- 1) Fujita, H., Yokosawa, H., Iwata, S. and Takahama, H., "Turbulent Flow in a Square Duct with Roughened Walls on Two Opposite Sides (1st Report, Measurement of Flow Velocities and Turbulent Stresses)," Trans. Japan Soc. Mech. Eng. (in Japanese), Vol. 52, No. 482 (1986), 3491.
- 2) Fujita, H., Yokosawa, H., Hirota, M. and Nishigaki, S., "Fully Developed Turbulent Flow in a Square Duct with a Rough Wall," Trans. Japan Soc. Mech. Eng. (in Japanese), Vol. 53, No. 492 (1987), 2370.
- 3) Fujita, H., Yokosawa, H., Hirota, M., and Nagata, C., "Fully Developed Turbulent Flow and Heat Transfer in a Square Duct with Two Roughened Facing Walls," Chem. Eng. Comm., Vol. 74 (1988), 95.
- 4) Brundrett, E. and Burroughs, P. R., "The Temperature Inner-Law and Heat Transfer for Turbulent Air Flow in a Vertical Square Duct," Int. J. Heat Mass Transf., Vol. 10 (1967), 1133.
- 5) Holman, J.P., "Heat Transfer 5th ed.," (1981), McGraw-Hill, New York, 294.
- 6) Tavoularis, S., "Techniques for Turbulence Measurement," Encyclopedia of Fluid Mechanics, Vol. 1, ed. N.P. Chermisinoff, (1986), Gulf Publishing Company, Houston, 1207.
- 7) Nieuwvelt, C., Bessem, J.M. and Trines, R.M., "A Rapid Thermometer for Measurement in Turbulent Flow," Int. J. Heat Mass Transf., Vol. 19, (1976), 975.
- 8) Colburn, A.P., "A Method of Correlating Forced Convection Heat Transfer Data and a Comparison with Fluid Friction," Trans. AIChE, Vol. 29, (1933), 174.
- 9) Sieder, E.N., and Tate, C.E., "Heat transfer and Pressure Drop of Liquids in Tubes," Ind. Eng. Chem., Vol. 28, (1936) 1429.
- 10) Brundrett, E., "Modified Hydraulic Diameter for Turbulent Flow," Turb. Forced Convect. Channel Bundles, Vol. 1, ed. S. Kakac and D.B. Spalding, (1978), Hemisphere, New York, 361.
- 11) Hishida, M., Nagano, Y. and Shiraki, A., "Structure of Turbulent Temperature and Velocity Fluctuations in the Thermal Entrance Region of a Pipe," Trans. Japan Soc. Mech. Eng. (in Japanese), Vol. 44, No. 385 (1978), 3145.